RESEARCH ARTICLE | SEPTEMBER 23 2025

Substrate effects on phase formation and interfacial stability in superconducting vanadium silicide thin films

Miguel Manzo-Perez ; Moeid Jamalzadeh ; Sooyeon Hwang ; Iliya Shiravand ; Kim Kisslinger ; Dmytro Nykypanchuk ; Davood Shahrjerdi

Appl. Phys. Lett. 127, 122601 (2025)
https://doi.org/10.1063/5.0291576
CHORUS

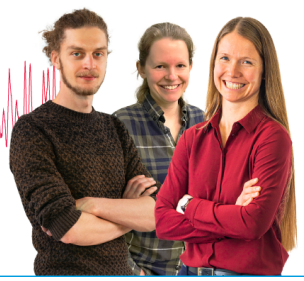

Applied Physics Letters ARTICLE pubs.aip.org/aip/apl

Substrate effects on phase formation and interfacial stability in superconducting vanadium silicide thin films

Cite as: Appl. Phys. Lett. **127**, 122601 (2025); doi: 10.1063/5.0291576
Submitted: 18 July 2025 · Accepted: 23 August 2025 ·
Published Online: 23 September 2025

Miguel Manzo-Perez,[1] Moeid Jamalzadeh,[1] Sooyeon Hwang,[2] Iliya Shiravand,[1] Kim Kisslinger,[2] Dmytro Nykypanchuk,[2] and Davood Shahrjerdi[1,a)]

AFFILIATIONS

[1]Electrical and Computer Engineering, New York University, Brooklyn, New York 11201, USA
[2]Center for Functional Nanomaterials, Brookhaven National Laboratory, Upton, New York 11973, USA

[a)]Author to whom correspondence should be addressed: davood@nyu.edu

ABSTRACT

Thin films of vanadium silicide (V-silicide) in the A15 cubic phase (V_3Si) are promising for superconducting quantum devices due to their high transition temperature and potential compatibility with scalable semiconductor fabrication. However, solid-phase synthesis often yields secondary silicide phases that degrade performance. Here, we investigate the influence of substrate properties using two silicon-on-insulator architectures: one with a polycrystalline HfO_2 buried layer (group A) and the other with amorphous SiO_2 (group B). Both systems exhibit superconductivity consistent with V_3Si formation, yet structural analysis reveals mixed-phase films in both cases. Crucially, only group A maintains an atomically sharp and chemically stable interface, a prerequisite for phase purity. Prolonged annealing in group A reduces the unwanted V_5Si_3 phase but also leads to the emergence of Si-rich VSi_2, likely due to localized substrate degradation. Preliminary atomic-resolution imaging suggests that HfO_2 crystallinity may promote local phase-selective nucleation. These findings highlight the importance of substrate design in promoting phase control and maintaining interfacial integrity in superconducting silicides.

A promising approach to scalable quantum technology involves developing superconducting materials compatible with standard semiconductor fabrication. Transition metal silicide thin films, long used in silicon (Si) electronics for low-resistance contacts,[1–5] offer significant potential due to their superconducting phases,[6–8] and compatibility with Si chip manufacturing (i.e., CMOS processes). Among these, vanadium silicide (V-silicide) in the A15 cubic phase (V_3Si) is particularly compelling. Its relatively high superconducting transition temperature (T_c), exceeding 10 K,[9–13] makes it a strong candidate for quantum devices that can operate at temperatures above the conventional millikelvin (mK) regime.

Despite this promise, synthesis of phase-pure V_3Si remains a significant material challenge. The solid-phase reaction between vanadium (V) and Si, while compatible with semiconductor manufacturing, typically yields multi-phase films. Additional secondary silicide phases such as VSi_2 and V_5Si_3 often form more readily[14–16] due to their lower formation energies, thereby reducing the phase purity and limiting superconducting performance. Although various strategies have been explored to suppress these secondary phases,[13,15,17] precise control over phase selectivity remains elusive.

Substrate properties, including chemical reactivity, structural integrity, and crystallinity, represent a largely underexplored dimension in controlling V-silicide phase formation. SiO_2, the most commonly used substrate,[11,13,15–19] is known to chemically react with V during annealing,[13,15,17,19] providing oxygen (O) and excess Si. By supplying additional Si, this interfacial decomposition is expected to alter local stoichiometry.[15,17,19] The release of O has also been reported to disrupt the formation of the V_3Si phase.[16] Therefore, substrates that do not supply Si or O may offer a more promising route to achieving phase-pure V_3Si. Nonetheless, the influence of alternative substrate materials has received comparatively limited attention in the context of V-silicide solid-phase synthesis.

In a pioneering study, Psaras *et al.* examined V-silicide solid-phase synthesis on two substrates: crystalline Al_2O_3 (sapphire) and amorphous SiO_2. They found that annealing V on sapphire led to a near-complete transformation from V_5Si_3 to V_3Si after prolonged annealing, an effect that was not observed on SiO_2.[15] However, these conclusions were based solely on bulk compositional characterization and lacked both superconducting measurements and atomic-resolution imaging, leaving the atomistic mechanism unresolved.

These findings suggest that chemically inert interfaces facilitate the transformation of existing secondary phases into V_3Si by reducing the likelihood of additional secondary phase formation. Another open question is whether crystalline substrates serve as templates in phase-selective growth. Notably, Psaras *et al.* also reported structural degradation of the sapphire substrate after extended annealing, highlighting the challenge of identifying substrates that can simultaneously enable phase purity and maintain structural integrity.

Motivated by these observations, we hypothesize that achieving phase-pure V_3Si requires substrates that are both chemically inert (i.e., not contributing O or excess Si to the reaction) and structurally stable under high-temperature annealing. We further posit that substrate crystallinity may promote selective phase nucleation by templating the growth of specific silicide structures. To test this, we designed a model system based on silicon-on-insulator (SOI) architecture incorporating a buried HfO_2 layer. HfO_2 was selected for its chemical inertness, thermal stability, and ability to form a polycrystalline structure at CMOS-compatible temperatures. We compared these engineered substrates (group A) to conventional SOI with SiO_2 buried oxide (group B) under identical synthesis conditions. Both groups exhibited superconducting transitions consistent with V_3Si formation, but structural characterization revealed multiphase V-silicide formation in both cases. Crucially, only the HfO_2-based samples maintained an atomically sharp interface under moderate annealing conditions and exhibited signs of templated phase growth. These findings highlight the critical role of substrate design in controlling phase evolution and maintaining interfacial integrity in V-silicide superconductors.

We assessed the influence of substrate properties on solid-phase V-silicide synthesis and interfacial stability by comparing two SOI-based designs: one with a buried polycrystalline HfO_2 layer (group A) and the other with amorphous SiO_2 (group B). Figure 1 illustrates the solid-phase synthesis procedure for V-silicide films, adapted from Zhang *et al.*[11] The process began with depositing a ~90 nm V layer onto an SOI substrate [Fig. 1(a)], followed by vacuum annealing at mid-10^{-6} Torr [Fig. 1(b)]. The V layer thickness significantly exceeds that of the top Si layer, intending to drive the reaction toward metal-rich silicide phases. Post annealing, the resulting structure [Fig. 1(c)] consists of a polycrystalline V-silicide film (highlighted in yellow), covered by a residual V layer partially oxidized to VO_x. Full synthesis details are provided in supplementary material Note S1.

Group A employed custom-engineered SOI wafers incorporating a buried HfO_2 layer beneath the top Si [Fig. 1(d)]. The buried stack consisted of $SiO_2/HfO_2/SiO_2$ (2/6/6 nm), with the top 2 nm SiO_2 buffer layer included to suppress Hf-silicide formation during substrate fabrication (see supplementary material Note S2). HfO_2 crystallizes readily in a polycrystalline monoclinic phase under CMOS-compatible conditions,[20] providing a structurally ordered, chemically inert interface for silicide growth.

Group B used commercial SOI substrates with a 15 nm top Si layer and a 145 nm SiO_2 buried oxide. The thicker oxide in group B was intentionally selected to sustain substantial interfacial reaction between SiO_2 and V, allowing focused investigation of how SiO_2 instability influences the V-silicide film formation. Notably, we observed oxide consumption exceeding 10 nm even under moderate synthesis conditions (supplementary material Note S3, Fig. S1). Both groups were processed under identical synthesis conditions, enabling a controlled comparison of how substrate reactivity and crystallinity influence V-silicide phase formation and interface integrity.

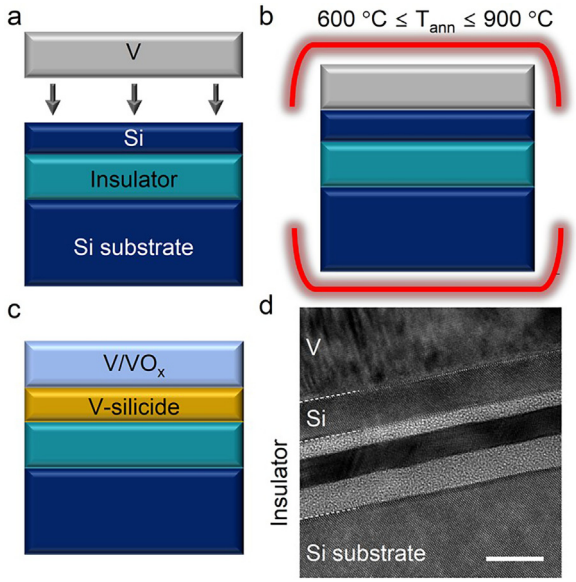

FIG. 1. V-silicide synthesis. The solid-phase reaction involves two main steps: (a) deposition of V onto the SOI substrate, and (b) annealing in high vacuum. The schematic in (c) illustrates the final structure, consisting of V-silicide capped with residual V/VO_x. (d) Cross-sectional TEM image of the engineered SOI substrate with a multilayer insulator, comprising $SiO_2/HfO_2/SiO_2$. Scale bar 10 is nm.

We first examined how the annealing temperature (T_{ann}) influences the formation of the V_3Si phase. Samples were annealed from 600 to 900 °C for 15 min. Since the presence of non-superconducting phases reduces the superconducting volume fraction, we used T_c as a proxy for V_3Si content, with higher T_c values suggesting its greater phase purity. Resistance was measured using the standard lock-in method in a closed-cycle cryostat (base temperature of 1.5 K), with current bias kept below 1 μA to avoid Joule heating (see supplementary material Note S4 for details). We define normalized resistance (R_{norm}) as the resistance at a given temperature divided by its value at 20 K, and extract midpoint T_c ($T_{c,mid}$) at $R_{norm} = 0.5$.

Figure 2(a) shows representative R_{norm} traces for the highest-performing samples from each group. The maximum $T_{c,mid}$ values reached 13.2 K for group A and 13.8 K for group B. These comparable values indicate that both substrate types can support V_3Si formation under these synthesis conditions, though they may differ in structural quality and stability, as examined later.

Figure 2(b) shows the evolution of $T_{c,mid}$ with annealing temperatures. Films annealed at 600 °C exhibited no superconductivity down to the cryostat base temperature of 1.5 K, indicating the absence of V_3Si formation. Superconductivity transitions appeared at 650 °C, consistent with the reported onset of V_3Si phase formation in this system.[11] In group B (SiO_2), $T_{c,mid}$ increased steadily with T_{ann} and peaked at 800 °C before declining slightly at 900 °C. In contrast, group A (HfO_2) achieved its highest $T_{c,mid}$ of 13.2 K at a lower annealing temperature of 700 °C. We observed a slight drop in $T_{c,mid}$ to 12.2 K at 800 °C, followed by an increase at 900 °C. This degradation in T_c appears to coincide with signs of structural damage to the buried HfO_2 layer (supplementary material Note S5, Fig. S5). We surmise that such damage might initially increase the volume fraction of secondary

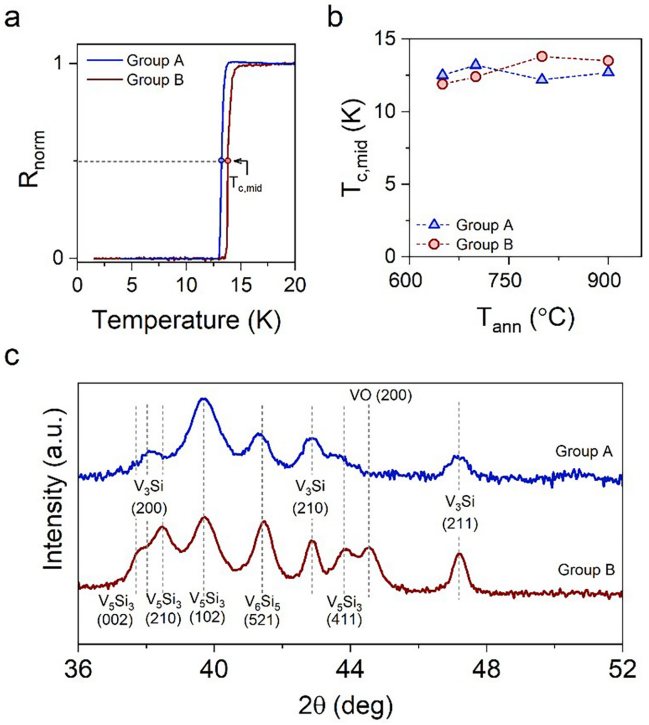

FIG. 2. Evidence of A15 V_3Si phase formation. (a) Four-point resistance vs temperature traces for representative samples from groups A and B, showing $T_{c,mid}$ (marked by circles) of 13.2 and 13.8 K, respectively. (b) Dependence of T_c on annealing temperature. (c) Corresponding powder XRD patterns for groups A and B samples prepared under similar synthesis conditions to those in panel (a), confirming the presence of the A15 V_3Si phase along with additional secondary phases in both groups.

phases and then partially convert into the desired V_3Si phase when annealing at 900 °C. Full understanding of this observation will require future investigation into the structural evolution of the V-silicide films synthesized under these conditions.

Assuming full conversion of Si to stoichiometric V_3Si, the resulting film thickness is expected to be approximately 2.1 times the original Si layer,[11] yielding ∼15 nm for group A and ∼30 nm for group B. These thicknesses exceed the superconducting coherence length of V_3Si (4–7 nm),[11,12] suggesting the potential for bulk-like superconducting behavior. However, the measured T_c values remain below the previously reported bulk value of 17.1 K,[9,10] consistent with the presence of unwanted V-silicide phases that can degrade superconductivity. To investigate the origin of this deviation, we performed structural analysis of the films, focusing on (1) phase composition, (2) interfacial stability, and (3) the potential influence of HfO_2 crystallinity on silicide texture.

Figure 2(c) shows x-ray diffraction (XRD) spectra for samples from groups A and B, annealed under similar conditions to their counterparts in Fig. 2(a). Both spectra exhibit clear peaks attributable to V_3Si, confirming its formation in both systems. Additional diffraction peaks correspond to secondary V-silicide phases, including V_6Si_5 and V_5Si_3, based on reference patterns. However, significant peak overlap, common in multiphase silicide systems, may obscure contributions from certain crystalline orientations. As such, the phase composition inferred from XRD should be interpreted with caution, and direct comparisons of phase purity between the two samples may not be fully conclusive based on XRD alone.

Having established the presence of V_3Si through electronic transport and XRD, we next used transmission electron microscopy (TEM) to examine the structural and interfacial properties of the films. Figure 3(a) shows a representative cross section from a group B sample (buried SiO_2), annealed at 730 °C. TEM imaging reveals pronounced interfacial intermixing between the V-silicide layer and the SiO_2 substrate, marked by localized disruptions in grain structure (see supplementary material Note S3 for additional details, Fig. S2). In these regions, secondary grains are observed beneath the primary columnar grains, indicating a sequential growth mechanism, where the initial silicide formation is followed by additional V-Si reaction driven by Si and O released from decomposing SiO_2. This interfacial instability is consistent with prior reports on the chemical reactivity of SiO_2.[13,15,16,21]

In contrast, TEM imaging of group A samples prepared at 700 °C reveals structurally distinct behavior. As shown in Fig. 3(b), V-silicide grains grow in a columnar fashion with no visible interfacial roughness or secondary grain formation. Scanning transmission electron microscopy with energy-dispersive x-ray spectroscopy [STEM-EDS, Fig. 3(c)] confirms a chemically abrupt interface between the V-silicide layer and HfO_2, with no evidence of interdiffusion. This is further supported by uniform Si signal intensity in EDS across the film (supplementary material Figs. S3 and S4). In stark contrast, the group B samples exhibit Si-rich regions within the silicide layer near the interface with the buried SiO_2 layer, likely due to additional Si supplied during the SiO_2 decomposition (see supplementary material Fig. S2).

To assess phase composition, we analyzed the V:Si ratio using EDS (supplementary material Figs. S2 and S3). The results suggest near-stoichiometric values consistent with V_3Si in both groups. While previous studies have used EDS to support the presence of V_3Si, we caution against over-interpretation of these results. The silicide grains are nanoscale and span multiple phases, as we demonstrate next. Since EDS analysis averages signals over multiple grains, the resulting elemental ratios may not reliably determine phase purity or identify specific phases. Nonetheless, EDS can provide useful insight into interfacial sharpness and overall elemental uniformity, particularly in comparing substrate reactivity of SiO_2 and HfO_2 (see supplementary material Notes S3 and S5).

Compositional characterization by Psaras *et al.*,[15] indicated near-complete transformation from V_5Si_3 to V_3Si on sapphire substrates after prolonged annealing (up to 240 min). We observed a similar trend in group A samples subjected to prolonged annealing at 800 °C. Comparison of XRD spectra for 60- and 240-min anneals [Fig. 3(d)] reveals a slight increase in V_3Si peak intensity accompanied by a marked reduction in V_5Si_3 peak intensity. The apparent correlated improvement in T_c supports this structural evolution and suggests that the prolonged annealing reduces the volume fraction of the non-superconducting V_5Si_3 phase. Nevertheless, T_c still remained well below the value expected for bulk V_3Si (17.1 K).[9,10]

Although the precise mechanism remains unclear, we attribute this limitation to interfacial degradation in group A substrates [Figs. 3(e) and 3(f)], which likely facilitates additional Si incorporation from the substrate at damaged sites. This interpretation is supported by the presence of the VSi_2 phase in these samples, as identified by XRD. The

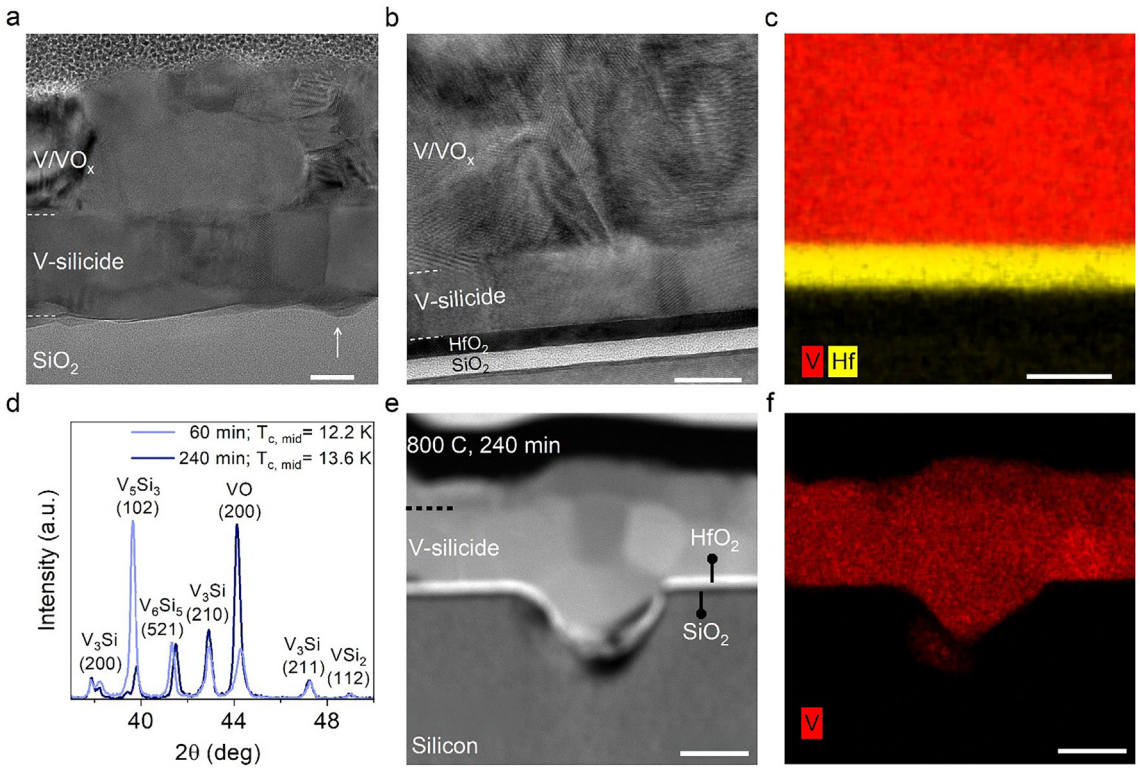

FIG. 3. Effect of buried oxide on interfacial stability. (a) Bright-field cross-sectional TEM image of V-silicide formed on group B substrates (SiO_2 insulator), showing significant interfacial intermixing and disrupted grain ordering along the film thickness. (b) TEM image for a group A sample annealed at 700 °C, revealing a sharp interface and columnar V-silicide grains. (c) EDS elemental maps of the sample in (b), confirming the chemical stability and interfacial integrity of the V-silicide/HfO_2 interface. (d) XRD patterns of two samples from group A, showing marked reduction in V_5Si_3 phase after prolonged annealing. This trend appears to coincide with the increase in T_c. (e) Cross section STEM image and (f) corresponding EDS elemental map of V for a group A sample annealed at 800 °C, revealing damage to the buried HfO_2 layer. Scale bars in (a) and (b) are 20 nm, (c) is 10 nm, and (e) and (f) are 60 nm.

resulting local change toward a Si-rich stoichiometry may counteract the benefits of improved phase purity elsewhere in the film. The observed substrate damage is reminiscent of the sapphire degradation reported by Psaras *et al.*,[15] highlighting the challenge of substrate material design that can preserve the interfacial integrity under prolonged annealing conditions.

For grain-specific analysis of phase diversity and crystalline structure, atomic-resolution STEM is essential. Given the limitations of techniques like XRD and EDS in resolving individual phases of nanoscale grains, we examined single grains using zone-axis imaging and image simulations. These data allow us to directly identify specific silicide phases and orientations, offering deeper insight into microstructural heterogeneity and potential substrate effects.

We employed high-angle annular dark-field-STEM (HAADF-STEM) to identify the phase of individual V-silicide grains. Its sensitivity to atomic number (Z)[22,23] provides strong contrast for the HfO_2 layer and resolves the V-silicide structure primarily through the heavier V atoms (Z = 23) compared to Si (Z = 14). Figures 4(a) and 4(e) show representative grains of V_3Si and V_5Si_3 along the [001] and [101] zone axes, respectively. Inverse fast Fourier transform (iFFT) images, reconstructed from selected diffraction spots, are shown as insets to enhance lattice visualization. Simulated HAADF-STEM images [Figs. 4(b) and 4(f)] confirm that the identified phases and orientations match the experimental observations. This analysis highlights the mixed-phase nature of the films at the grain level, revealing a level of structural complexity not accessible through conventional measurements.

To further assess substrate/film interactions in group A, we examined the interface between V-silicide and HfO_2 at atomic resolution. Figures 4(c) and 4(g) present false-colored inverse FFT images extracted from the marked regions in Figs. 4(a) and 4(e), respectively. In both cases, the V_3Si and V_5Si_3 grains terminate sharply at the HfO_2 boundary, with no discernible interfacial mixing or intermediate phase. These results suggest that HfO_2 can support direct nucleation of multiple silicide phases while preserving structural and chemical integrity.

Let us now consider the potential role of crystalline HfO_2 in influencing the orientation and phase selection of V-silicide grains. Figures 4(d) and 4(h) show atomic models (generated using VESTA[24]) corresponding to the experimental images in Figures 4(c) and 4(g), employing a monoclinic HfO_2 phase. The extent of atomic alignment between the V_5Si_3 and the underlying HfO_2 in Fig. 4(g) is striking, raising the possibility that the substrate may play a role in templating the overlying film.

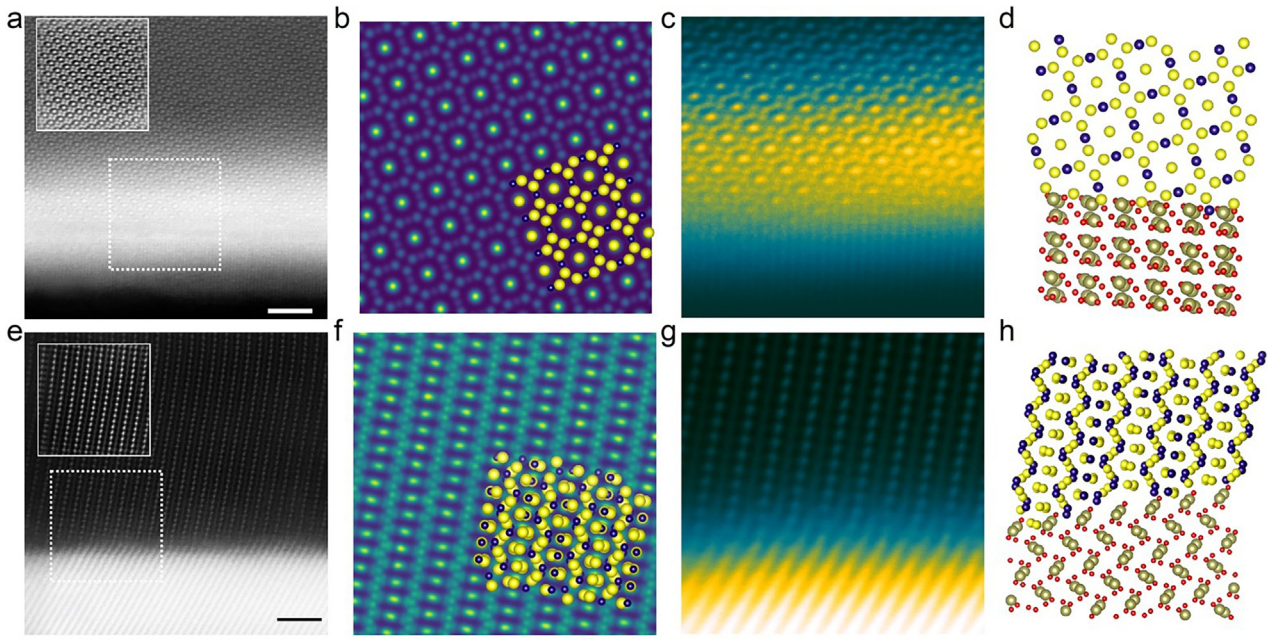

FIG. 4. Phase identification of individual V-silicide grain in group A samples. (a) and (e) Experimental HAADF-STEM images and (b) and (f) corresponding simulated HAADF-STEM images of the identified V_3Si and V_5Si_3 phases along the along the [001] and [101] zone axes, respectively. The scale bars are 2 nm. Insets outlined with solid squares in (a) and (e) show the iFFTs. Insets in (b) and (f) display the corresponding atomic models, with yellow and navy spheres representing V and Si atoms, respectively. (c) and (g) iFFTs extracted from the dotted squares in (a) and (e), showing atomically sharp interface between V-silicide and HfO_2. (d) and (h) Proposed atomic models of the interfaces shown in (c) and (g). Gold and red spheres indicate Hf and O, respectively.

In contrast, the structural relationship between HfO_2 and V_3Si in Fig. 4(c) remains inconclusive. To further explore this possibility, we identified and imaged additional V_3Si grains oriented along the [100] direction (Fig. 5). A comparison of two such grains reveals that their underlying HfO_2 exhibits similar in-plane d-spacings (0.17 and 0.18 nm) and comparable lattice angles relative to the bright atomic columns in the HAADF-STEM images (76° and 80°, respectively). These similarities, despite uncertainties from image distortions or projection effects, suggest that specific orientations of monoclinic HfO_2 may provide favorable interfacial conditions for the heterogeneous nucleation of V_3Si. Although the exact crystallographic identity of these HfO_2 grains could not be determined from the available data, these results point to a potentially important role of substrate crystallinity in guiding local structure during silicide formation. Further investigation is needed to reveal the relationship between monoclinic HfO_2 grain orientation and V-silicide phase selection.

We also examined individual V-silicide grains in Group B samples using atomic-resolution STEM (supplementary material Note S6, Figs. S6–S9). These analyses confirm the presence of multiple phases in group B samples, including V_3Si, V_5Si_3, and V_6Si_5. As expected, grains on SiO_2 substrates, due to their amorphous nature, show no orientational preference and exhibit frequent interfacial disruption, likely a consequence of interfacial reactions between SiO_2 and V during synthesis.

In conclusion, the findings of our study highlight key structural differences between V-silicide films synthesized on polycrystalline

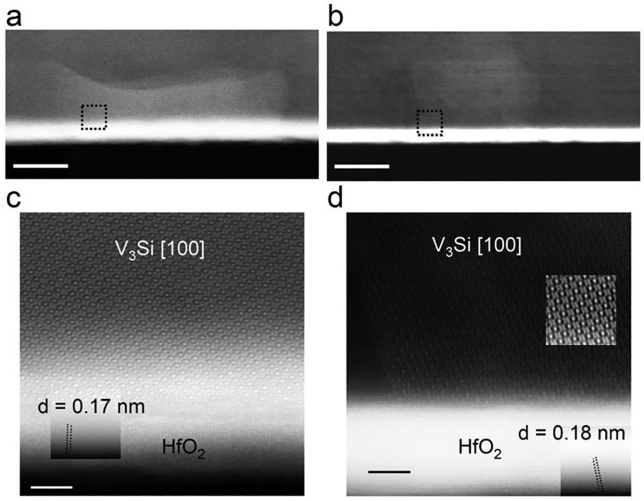

FIG. 5. Crystalline HfO_2 as a potential growth template for V_3Si formation. (a) and (b) Overview HAADF-STEM images with markers indicating the regions where the high-resolution images in (c) and (d) were acquired. Insets in (c) and (d) are iFFT results to enhance image clarity. The lattice-resolved images provide preliminary evidence that the underlying crystalline HfO_2 may influence the orientation and phase selection of V_3Si grains during nucleation. Scale bars in (a) and (b) are 20 nm and in (c) and (d) are 2 nm.

HfO_2 and amorphous SiO_2 substrates. The chemical stability of HfO_2 suppresses interfacial reactions with V during synthesis, maintaining atomically sharp substrate–film interfaces, in contrast to the degraded, Si-rich interfaces seen with SiO_2. Prolonged annealing in group A appears to enhance phase purity by reducing the amount of secondary V_5Si_3 phase. However, the emergence of the Si-rich VSi_2 phase, likely driven by local substrate degradation, partially counteracts this benefit. Finally, the polycrystalline structure of monoclinic HfO_2 appears to influence local grain alignment and support direct nucleation of specific V-silicide phases.

These results highlight the broader potential of chemically inert, thermally stable, and structurally ordered oxides for phase-selective synthesis of thin-film superconducting silicides. Future work combining grain-resolved orientation mapping and systematic substrate design will be essential to establish how substrate structure influences phase selection. Such insights may offer improved control over silicide interfaces and phase purity, advancing their integration into superconducting quantum device architectures.

See the supplementary material for details on group A substrate fabrication, the solid-phase synthesis process, and additional materials characterization data for the V-silicide films.

The authors acknowledge partial support from NSF Award No. 2216332. DS gratefully acknowledges Soitec for providing the commercial fully depleted silicon-on-insulator (FD-SOI) substrates, featuring a buried SiO_2 insulator, used in this study. This work was performed in part at the NYU Nanofabrication Cleanroom Facility (NYU Nanofab). This research used the Materials Synthesis and Characterization and Electron Microscopy facilities of the Center for Functional Nanomaterials (CFN), which is a U.S. Department of Energy Office of Science User Facility, at Brookhaven National Laboratory under Contract No. DESC0012704.

AUTHOR DECLARATIONS

Conflict of Interest

The authors have no conflicts to disclose.

Author Contributions

Miguel Manzo-Perez: Conceptualization (equal); Data curation (lead); Formal analysis (equal); Investigation (equal). **Moeid Jamalzadeh:** Data curation (supporting); Formal analysis (supporting); Investigation (supporting). **Sooyeon Hwang:** Data curation (equal); Formal analysis (equal). **Iliya Shiravand:** Data curation (supporting); Formal analysis (supporting). **Kim Kisslinger:** Data curation (equal); Formal analysis (supporting). **Dmytro Nykypanchuk:** Data curation (equal); Formal analysis (supporting). **Davood Shahrjerdi:** Conceptualization (equal); Formal analysis (equal); Funding acquisition (equal); Investigation (equal); Supervision (lead).

DATA AVAILABILITY

The data that support the findings of this study are available from the corresponding author upon reasonable request.

REFERENCES

[1]S.-L. Zhang and U. Smith, "Self-aligned silicides for Ohmic contacts in complementary metal–oxide–semiconductor technology: $TiSi_2$, $CoSi_2$, and NiSi," J. Vac. Sci. Technol., A **22**(4), 1361–1370 (2004).
[2]B. Froment, M. Muller, H. Brut, R. Pantel, V. Carron, H. Achard, A. Halimaoui, F. Boeuf, F. Wacquant, and C. Regnier, "Nickel vs. cobalt silicide integration for sub-50 nm CMOS," in *33rd Conference on European Solid-State Device Research (ESSDERC'03)* (IEEE, 2003), pp. 215–218.
[3]G. Larrieu, E. Dubois, X. Wallart, X. Baie, and J. Katcki, "Formation of platinum-based silicide contacts: Kinetics, stoichiometry, and current drive capabilities," J. Appl. Phys. **94**(12), 7801–7810 (2003).
[4]M. E. Alperin, T. C. Hollaway, R. A. Haken, C. D. Gosmeyer, R. V. Karnaugh, and W. D. Parmantie, "Development of the self-aligned titanium silicide process for VLSI applications," IEEE J. Solid-State Circuits **20**(1), 61–69 (1985).
[5]G. Van Gurp, "Cobalt silicide layers on Si. II. Schottky barrier height and contact resistivity," J. Appl. Phys. **46**(10), 4308–4311 (1975).
[6]T. R. Nanayakkara, A. T. Bollinger, R. Li, C. Zhou, A. K. Rumaiz, X. Tong, L. Zhang, K. Kisslinger, C. T. Black, and M. Liu, "Synthesis and electrical transport properties of superconducting platinum silicide thin films and devices," J. Vac. Sci. Technol., A **42**(6), 063407 (2024).
[7]S.-P. Chiu, C. Tsuei, S.-S. Yeh, F.-C. Zhang, S. Kirchner, and J.-J. Lin, "Observation of triplet superconductivity in $CoSi_2$/$TiSi_2$ heterostructures," Sci. Adv. **7**(29), eabg6569 (2021).
[8]K. Oto, S. Takaoka, K. Murase, and S. Ishida, "Superconductivity in PtSi ultrathin films," J. Appl. Phys. **76**(9), 5339–5342 (1994).
[9]G. F. Hardy and J. K. Hulm, "Superconducting silicides and germanides," Phys. Rev. **89**(4), 884 (1953).
[10]G. F. Hardy and J. K. Hulm, "The superconductivity of some transition metal compounds," Phys. Rev. **93**(5), 1004 (1954).
[11]W. Zhang, A. T. Bollinger, R. Li, K. Kisslinger, X. Tong, M. Liu, and C. T. Black, "Thin-film synthesis of superconductor-on-insulator A15 vanadium silicide," Sci. Rep. **11**(1), 2358 (2021).
[12]T. D. Vethaak, F. Gustavo, T. Farjot, T. Kubart, P. Gergaud, S.-L. Zhang, F. Lefloch, and F. Nemouchi, "Superconducting V_3Si for quantum circuit applications," Microelectron. Eng. **244–246**, 111570 (2021).
[13]M. Bose, D. L. Cortie, S. Rubanov, A. P. Le Brun, T. R. Finlayson, and J. C. McCallum, "In-situ investigation of V3Si phase formation at high temperature and resulting superconductivity," Appl. Surf. Sci. **696**, 162930 (2025).
[14]R. Pretorius, T. Marais, and C. Theron, "Thin film compound phase formation sequence: An effective heat of formation model," Mater. Sci. Rep. **10**(1–2), 1–83 (1993).
[15]P. Psaras, M. Eizenberg, and K.-N. Tu, "Sequential silicide formation between vanadium and amorphous silicon thin-film bilayers," J. Appl. Phys. **56**(12), 3439–3444 (1984).
[16]R. Schutz and L. Testardi, "The formation of vanadium silicides at thin-film interfaces," J. Appl. Phys. **50**(9), 5773–5781 (1979).
[17]G. i. Oya, H. Inabe, Y. Onodera, and Y. Sawada, "Superconducting transition temperatures of thin V_3Si layers formed by the interaction of V films with thinly oxidized Si wafers," J. Appl. Phys. **53**(2), 1115–1121 (1982).
[18]F. Nava, O. Bisi, and K.-N. Tu, "Electrical transport properties of V_3Si, V_5Si_3, and VSi_2 thin films," Phys. Rev. B **34**(9), 6143 (1986).
[19]K.-N. Tu, J. Ziegler, and C. Kircher, "Formation of vanadium silicides by the interactions of V with bare and oxidized Si wafers," Appl. Phys. Lett. **23**(9), 493–495 (1973).
[20]M.-Y. Ho, H. Gong, G. Wilk, B. Busch, M. Green, P. Voyles, D. Muller, M. Bude, W. Lin, and A. See, "Morphology and crystallization kinetics in HfO_2 thin films grown by atomic layer deposition," J. Appl. Phys. **93**(3), 1477–1481 (2003).
[21]O. Michikami and H. Takenaka, "V_3Si thin-film synthesis by magnetron sputtering," Jpn. J. Appl. Phys., Part 1 **21**(3A), L149 (1982).
[22]M. Drimmer, S. Telkamp, F. L. Fischer, I. C. Rodrigues, C. Todt, F. Krizek, D. Kriegner, C. Müller, W. Wegscheider, and Y. Chu, "The effect of niobium thin film structure on losses in superconducting circuits," arXiv:2403.12164 (2024).
[23]S. Pennycook and L. Boatner, "Chemically sensitive structure-imaging with a scanning transmission electron microscope," Nature **336**(6199), 565–567 (1988).
[24]K. Momma and F. Izumi, "VESTA: A three-dimensional visualization system for electronic and structural analysis," J. Appl. Crystallogr. **41**(3), 653–658 (2008).